Algal Research 49 (2020) 101937

Contents lists available at ScienceDirect

Algal Research

journal homepage: www.elsevier.com/locate/algal

Evaluation of diurnal responses of *Tetradesmus obliquus* under nitrogen limitation

G. Mitsue León-Saiki[a,1], Benoit M. Carreres[b,1], Ilse M. Remmers[a], René H. Wijffels[a,c], Vitor A.P. Martins dos Santos[b,d], Douwe van der Veen[a], Peter J. Schaap[b], Maria Suarez-Diez[b,2], Dirk E. Martens[a,*,1]

[a] Bioprocess Engineering, Wageningen University & Research, the Netherlands
[b] Laboratory of Systems and Synthetic biology, Wageningen University & Research, the Netherlands
[c] Nord University, Faculty of Biosciences and Aquaculture, N-8049 Bodø, Norway
[d] LifeGlimmer GmbH, Markelstrasse 38, 12163 Berlin, Germany

ARTICLE INFO

Keywords:
Microalgae
Scenedesmus obliquus
Starchless mutant
Diurnal transcription changes
Nitrogen limitation
Day/night cycles

ABSTRACT

Tetradesmus obliquus is an oleaginous microalga with high potential for triacylglycerol production. We characterized the biochemical composition and the transcriptional landscape of *T. obliquus* wild-type and the starchless mutant (*slm1*), adapted to 16:8 h light dark (LD) cycles under nitrogen limitation. In comparison to the nitrogen replete conditions, the diurnal RNA samples from both strains also displayed a cyclic pattern, but with much less variation which could be related to a reduced transcription activity in at least the usually highly active processes. During nitrogen limitation, the wild-type continued to use starch as the preferred storage compound to store energy and carbon. Starch was accumulated to an average content of 0.25 $g \cdot g_{DW}^{-1}$, which is higher than the maximum observed under nitrogen replete conditions. Small oscillations were observed, indicating that starch was being used as a diurnal energy storage compound, but to a lesser extent than under nitrogen replete conditions. For the *slm1* mutant, TAG content was higher than for the wild-type (average steady state value was 0.26 $g \cdot g_{DW}^{-1}$ for *slm1* compared to 0.06 $g \cdot g_{DW}^{-1}$ for the wild-type). Despite the higher TAG content in the *slm1*, the conversion efficiency of photons into biomass components for the *slm1* was only half of the one obtained for the wild-type. This is related to the observed decrease in biomass productivity (from 1.29 $g_{DW} \cdot L^{-1} \cdot day^{-1}$ for the wild-type to 0.52 $g_{DW} \cdot L^{-1} \cdot day^{-1}$ for the *slm1*). While the transcriptome of *slm1* displayed clear signs of energy generation by degrading TAG and amino-acids during the dark period, no significant variation of these metabolites could be measured. When looking through the diurnal cycle, the photosynthetic efficiency was lower for the *slm1* mutant compared to the wild-type especially during the second half of the light period, where starch accumulation occurred in the wild-type.

1. Introduction

Microalgae are considered as one of the most promising renewable sources for the production of feed, fuels and chemicals [1–3] However, in order to make large scale production of algal biodiesel economically feasible, high triacylglycerol (TAG) productivity are needed [3,4].

Tetradesmus obliquus (formerly known as *Scenedesmus obliquus* [5]) is a microalga of interest due to its high TAG content and the fact that it can retain a high photosynthetic efficiency under nitrogen starvation [6–9] Besides, de Jaeger et al. [10] developed the starchless mutant *slm1* that showed a higher maximum TAG yield on light compared to the wild-type (0.22 $g_{TAG} \cdot mol_{ph}^{-1}$ compared to 0.14 $g_{TAG} \cdot mol_{ph}^{-1}$), as well as a higher maximum TAG content (0.57 $g \cdot g_{DW}^{-1}$ compared to 0.45 $g \cdot g_{DW}^{-1}$) under batch nitrogen starvation and continuous illumination [11].

In large scale production, microalgal biomass first will be grown outdoors under favorable nitrogen replete conditions and light/dark cycles (LD). After biomass has been produced, the lipid production phase can be done under nitrogen deplete conditions. The behavior of *T. obliquus* under nitrogen replete conditions and diurnal 16:8 h light/

* Corresponding author.
E-mail address: dirk.martens@wur.nl (D.E. Martens).
[1] Authors contributed equally.
[2] The authors jointly supervised the work.

https://doi.org/10.1016/j.algal.2020.101937
Received 10 December 2019; Received in revised form 4 May 2020; Accepted 5 May 2020
Available online 25 May 2020

dark (LD) cycles has been previously studied [7,12]. Under such conditions, *T. obliquus* wild-type and starchless mutant *slm1* showed synchronized cell division and growth. *T. obliquus* wild-type showed diurnal oscillations in biomass composition, with an accumulation of starch during the light period that was consumed during the dark period and beginning of next light period. For the *slm1*, no such oscillations in biomass composition were found, which shows that this microalga does not need starch as a temporary energy storage compound to survive dark periods up to 12 h [13]. The lack of starch, however, did result in a reduction of the conversion of energy (photons) to biomass [7,13].

Under nitrogen deplete conditions, many microalgal species accumulate starch or TAG, which allows the capture and storage of energy and carbon that can be rapidly used when nitrogen becomes available again [14]. However, under deplete conditions growth stops, the photosynthetic efficiency rapidly decreases and also TAG production stops after a certain time. Since production of TAG occurs also under nitrogen limitation in combination with LD cycles, this may result in continuous production and in the end a higher yield of TAG on light. Consequently, the behavior of *T. obliquus* under these conditions is of interest. The average steady state behavior under nitrogen limitation and LD cycles of both *T. obliquus* wild type and *slm1* has been previously reported [15]. However, the detailed diurnal behavior during a single LD cycle under nitrogen limitation has not been studied in these strains. Therefore, the aim of this paper is to obtain a better understanding of the diurnal behavior of *T. obliquus* wild-type and starchless mutant *slm1* under nitrogen limitation, with focus on the diurnal changes in starch and TAG content, and on energy efficiency. Next to studying the biochemical composition and light use, gene expression was examined from RNA sequencing data to obtain more insight in the precise regulation in the affected pathways. These results will also be compared to the previously observed changes without nitrogen limitation [12].

2. Materials and methods

2.1. Strains, pre-culture conditions and cultivation medium

Wild-type *Tetradesmus obliquus* UTEX 393 was obtained from the Culture Collection of Algae, University of Texas. The starchless mutant of *T. obliquus* (*slm1*) was generated by de Jaeger et al. [10]. Pre-cultures were grown as described by León-Saiki et al. [7] in defined medium described by Breuer et al. [6].

2.2. Reactor set-up and experimental conditions

T. obliquus was continuously cultivated in a sterilized flat panel airlift-loop photobioreactor with a working volume of 1.7 L and a 0.02 m light path (Labfors 5 Lux, Infors HT, Switzerland). Temperature was maintained at 27.5 °C and pH was controlled at 7.0 by the automatic addition of 2.5% (v/v) H_2SO_4. The reactor was continuously sparged with 1 $L{\cdot}min^{-1}$ air enriched with 2% CO_2. Light was provided by a light panel with 260 LEDs with a warm white spectrum at an incident photon flux density of 500 $\mu mol{\cdot}m^{-2}{\cdot}s^{-1}$ in a 16:8 h light/dark (LD) block cycle. The reactor was inoculated to an optical density (OD_{750}) of 0.1.

Duplicate turbidostat cultivations were done, where the light intensity at the rear of the reactor was kept constant at 10 $\mu mol{\cdot}m^{-2}{\cdot}s^{-1}$ by addition of medium. Dilution medium [6] was prepared without KNO_3 and KNO_3 was separately fed at 0.075 $g_N{\cdot}L^{-1}\,day^{-1}$ for the wild-type and 0.052 $g_N{\cdot}L^{-1}\,day^{-1}$ for the *slm1*. This corresponds to a nitrogen limitation of 30% of the nitrogen consumption rate observed under nitrogen replete and light limitation [15]. Dilution medium was only added during the light period and switched off during the night. This type of system allows the study of the interaction between growth, nitrogen consumption and lipid accumulation [16].

Cultures were allowed to reach steady state, which was defined as a constant biomass concentration and daily dilution rate for a period of at least 3 days. After steady state was reached, liquid samples were freshly taken from the reactor and either immediately used for dry weight measurements or centrifuged for 5 min at 2360 $\times g$ for biochemical analysis (approximately 10–12 mg for proteins, 5 mg for starch, 7 mg for triacylglycerols (TAG) and 5 mg for total carbohydrates). In addition, at least three daily overflow samples were collected for each strain. Due to restrictions on working hours of the laboratory, the samples were collected in two successive time settings to allow sampling the dark period during the day. After collecting samples of the first half of the cycle, light settings were shifted and the culture was then allowed to reach oscillating steady-state before collecting samples for the second half of the cycle. The first and the last samples of each time settings are overlapping samples for control.

2.3. Dilution rate

Dilution rate was calculated by measuring the feed of the dilution medium (without KNO_3) and the feed of the KNO_3 medium over intervals of 10 min. Dilution rates were then calculated as the total medium added over 30 min divided by the reactor volume. After that, a moving average of 60 min was done.

2.4. Measurements

Dry weight (DW) concentration was determined as described by Kliphuis et al. [17]. Total carbohydrates were determined according to DuBois et al. [18] and Herbert et al. [19] using glucose as a standard. Starch content was measured as described by De Jaeger et al. [10] using a total starch kit (K-TSTA-100A, Megazyme, Ireland). Triacylglycerol (TAG) content was quantified as described by Remmers et al. [15] using glyceryl trinonadecanoate (T4632; Sigma Aldrich, Netherlands) and 1,2-dipentadecanoyl-sn-glycero-3-phospho-(1′-rac-glycerol) (sodium salt) (840446, Avanti Polar Lipids Inc., U.S.) as internal standards. Total protein concentration was measured done using a colorimetric assay (Bio-Rad DC protein assay, 5000116, Bio-Rad, U.S.) as described by Postma et al. [20].

2.5. Conversion of photons into biomass

The theoretical amount of photons converted into biomass was calculated based on the theoretical photon requirements for the biomass components (1.33 $g{\cdot}mol_{ph}{}^{-1}$ for TAG, 3.24 $g{\cdot}mol_{ph}{}^{-1}$ for starch, and 1.62 $g{\cdot}mol_{ph}{}^{-1}$ for functional biomass) [17,21] and the photon absorption rate (1.36 $mol_{ph}{\cdot}L^{-1}{\cdot}day^{-1}$) [7]. Samples were taken in intervals of 3 h. For the calculation of the hourly energy conversion efficiency the additional points for biomass composition were estimated assuming a proportional change between the measured points. Biomass composition of the overflow samples (collected during 24 h on ice) was used to calculate the average steady state values.

2.6. Starch and TAG productivities

The starch productivity ($r_{starch,t}$ in $g{\cdot}L^{-1}{\cdot}h^{-1}$) was calculated using a balance for starch over short time intervals using Eq. (1):

$$\frac{dC_{starch}}{dt} = -D_t \bullet C_{starch,t} + r_{starch,t} \quad (1)$$

where D_t (h^{-1}) is the dilution rate at time t (see Section 2.3 for calculation), $C_{starch,t}$ ($g{\cdot}L^{-1}$) is the starch concentration on time t, which is calculated by multiplying the biomass concentration (g·L)with the starch content of biomass ($g{\cdot}g^{-1}$) as measured at time t and ($\frac{dC_{starch}}{dt}$) ($g{\cdot}L^{-1}{\cdot}h^{-1}$) is the accumulation rate of starch calculated over a 3 hour period according to:

$$\frac{dC_{starch}}{dt} = \frac{C_{starch}(t) - C_{Starch}(t - 3\,\mathrm{h})}{3\,\mathrm{h}} \quad (2)$$

The TAG productivity was calculated in a similar way where the changes in TAG content over intervals of 3 h ($\frac{dC_{TAG}}{dt}$), the dilution rate (D_t in h^{-1}), and the TAG content ($C_{TAG,t}$ in $g{\cdot}L^{-1}$) were used. During the dark period the dilution rate is zero and the productivity is determined by the accumulation term only.

2.7. RNA sampling, extraction, and sequencing

After steady state was reached, 8 mL samples were taken for RNA extraction (approximately 10 mg_{DW}). Cells were immediately collected by centrifugation (4255 × *g*, 0 °C for 5 min), supernatant was discarded and pellets were frozen in liquid nitrogen and stored at −80 °C until further extraction. Samples for RNA extraction were taken in intervals of 3 h for both the wild-type and the *slm1* mutant. Sampling strategy and RNA extraction were performed as described in our previous study [12].

2.8. Analysis of RNA expression

The RNA-seq samples were treated and analyzed with the same method as our previous study [12]. To summarize, the expression was calculated by aligning the read samples over the available genome of *T. obliquus* UTEX-393 [22]. From the aligned samples, Fragments Per Kilobase of transcripts per Million reads mapped (FPKM) values were computed and used in the following steps. Genes with significant changes of expression over time were identified using maSigPro [23]. These genes were then separated using hierarchical clustering and Pearson's correlation. The optimal number for cluster separation was determined by combining the results from seven indexes commonly used for this purpose. These indexes were calculated using the functions of "clusters.stats" from the "fpc" R package [24]. Functional characterization of genes in each cluster was done using the functional annotation presented in [12]. Again, the same methods were applied to determine the enrichment of clusters in GO terms and in KEGG pathways [12]. In brief, enrichment analyses were performed using the hypergeometric function to model the background probability density. Enzyme commission (EC) numbers were associated to metabolic pathways using KEGG pathways maps. Pathways fitting the following requirements were kept for further analysis: 60% coverage if 3 to 6 EC numbers annotated, and 50% coverage if 6 to 10 EC numbers annotated, and 25% of coverage if > 10 EC numbers were annotated. Enrichments with a p-value lower than 0.05 were considered significant. For the GO enrichment analysis multiple test correction was performed using the Benjamini-Hochberg procedure. Enrichments with FDR < 0.05 were considered significant.

The annotation was curated manually for specific reactions related to starch, lipids and TAG synthesis and degradation pathways. To do so, the combination of top score and p-value from Enz-DP were considered, as well as the relative difference between the scores, and as a final verification, the proteins were aligned using DELTA-Blast and HMMER3.

3. Results and discussion

3.1. Growth of Tetradesmus obliquus wild-type and slm1

Our experimental set-up using turbidostat controlled systems imposes a fixed light uptake. We created an energy imbalance by decreasing the nitrogen supply rate to 30% of the value that would be needed to have nitrogen replete growth at the fixed light uptake rate.

Nitrogen limitation resulted in a reduced growth rate (Fig. 1). Nitrogen limited cultures showed a diurnal pattern in dilution rate (D), with both the wild-type and the starchless mutant *slm1* showing a similar pattern. Dilution patterns were, however, different from those under nitrogen replete conditions, specifically with respect to the start of dilution after the light went on and the moment where the maximum dilution rate was reached. Dilution started about 4 h after start of the light period under nitrogen limitation, while under nitrogen replete conditions dilution started immediately after the beginning of the light period. As a result, the time at which the maximum dilution rate was reached was also shifted and was reached at 7 h. A possible explanation for this shift may be that, as nitrogen was not added during the night, nitrogen content was equal to zero (starvation). This may have resulted in cells being unable to prepare for the next day, or cells switching to a nitrogen starvation mode, breaking down proteins and pigments, from which they had to recover. With respect to the first case, it is possible that cells prepare during the night for the next day so they can start growing quickly. If nitrogen is needed for this preparation, cells would have to first fixate nitrogen when the light is on, which would explain the delay. With respect to the second case, cells switch to a nitrogen starvation mode, stopping pigment synthesis and breaking down pigments and proteins, which would result in a decreased pigment content at the beginning of the light period. This last point is supported by the fact that the light out for the wild-type was 1 $\mu mol{\cdot}m^{-2}{\cdot}s^{-1}$ above set-point, indicating breakdown of light absorbing material. Consequently, first a certain amount of pigment has to be synthesized before the light out drops below the set-point and dilution starts. For *slm1*, an oscillatory pattern was observed (Fig. 1B), which was also observed in our previous study in nitrogen replete conditions [12].

Under favorable nitrogen replete conditions, oleaginous microalgae produce only small amounts of TAG, while under unfavorable nitrogen starvation conditions, TAG accumulation is induced and contents of up to 0.40 $g{\cdot}g_{DW}^{-1}$ can be reached [25,26] However, this unfavorable environmental conditions come with the disadvantage of a complete stop of cell division [15]. Nitrogen limitation processes were suggested as an attempt to overcome the disadvantages observed under nitrogen starvation [16]. As observed for *T. obliquus*, growth still occurs under nitrogen limitation, but this is reduced to approximately half of the one observed under nitrogen replete conditions (from 1.12 ± 0.01 day^{-1} under nitrogen replete [7] to 0.55 ± 0.07 day^{-1} under nitrogen limitation). This was also observed for other microalgae, such as *Neochloris oleoabundans* [4]. For the starchless mutant *slm1* the 24 h average daily dilution rate, i.e. growth rate, was reduced even more (from 0.90 ± 0.01 day^{-1} under nitrogen replete to 0.22 ± 0.02 day^{-1} under nitrogen limitation), showing again the reduction in growth and lower photosynthetic efficiency when blocking starch production.

3.2. Diurnal changes of storage compounds: starch and TAG

During nitrogen limitation, starch continued to be the preferred storage compound to store energy and carbon for the wild-type (Fig. 2A). Starch was accumulated to an average content of 0.25 $g{\cdot}g_{DW}^{-1}$, with a maximum content of approximately 0.29 $g{\cdot}g_{DW}^{-1}$, which is higher than the maximum observed under nitrogen replete conditions (0.20 $g{\cdot}g_{DW}^{-1}$) [7]. The overall preference of *T. obliquus* wild-type towards storing starch has been previously observed [11,15]. When looking into the starch content during the diurnal cycle, a small oscillation can be observed (Fig. 2A), where starch content slightly increases between 9 and 12 h and decreases during the dark period. This can also be seen in the starch productivity shown in Fig. 2C, that was calculated according to Eq. (1). Starch productivity remained positive just above zero during the first 9 h, then increased reaching the maximum value on t = 12 h after which the starch productivity decreased and became negative at t = 21 h, indicating consumption.

Under nitrogen replete conditions, TAG is not accumulated, whereas under nitrogen limitation or starvation substantial amounts of TAG can be accumulated in *T. obliquus*, as observed by Remmers et al. [15]. However, no information is known on the diurnal role of this compound under nitrogen limitation in *T. obliquus*. Therefore, we also measured

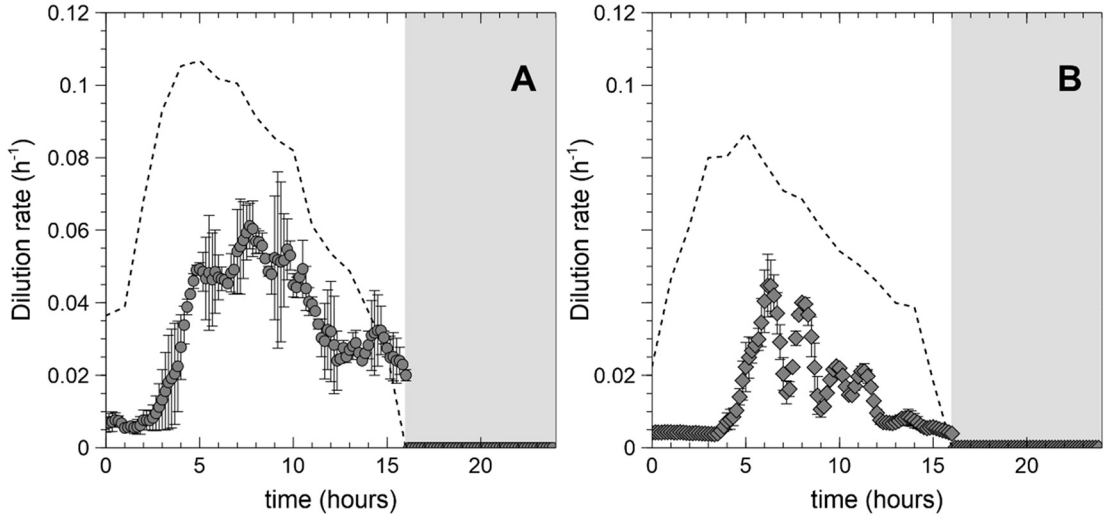

Fig. 1. Changes in dilution rate for *Tetradesmus obliquus* wild-type (A) and slm1 (B) under nitrogen limitation. Values represent the average of replicate reactors and error bars represent minimum and maximum values (n = 2). The x axis shows hours after start of light period. Shaded areas indicate the dark period. The dotted line is the average dilution rate from the N-replete cultures (n = 2 for each strain) as taken from León-Saiki et al. [7].

the TAG content during the diurnal cycle in intervals of 3 h. The wild-type showed a constant content of approximately 0.07 $g \cdot g_{DW}^{-1}$ for all measured time points (Fig. 2A). This rather low content of TAG can be explained by the fact that carbon and energy are mainly stored as starch. TAG is only formed if the carbon and energy supply exceeds the storage capacity in starch, as also mentioned in literature [11,15,27]. For *T. obliquus*, Remmers et al. [15] found that TAG is only accumulated after starch reaches its cellular maximum of 0.40 $g \cdot g_{DW}^{-1}$. Under this

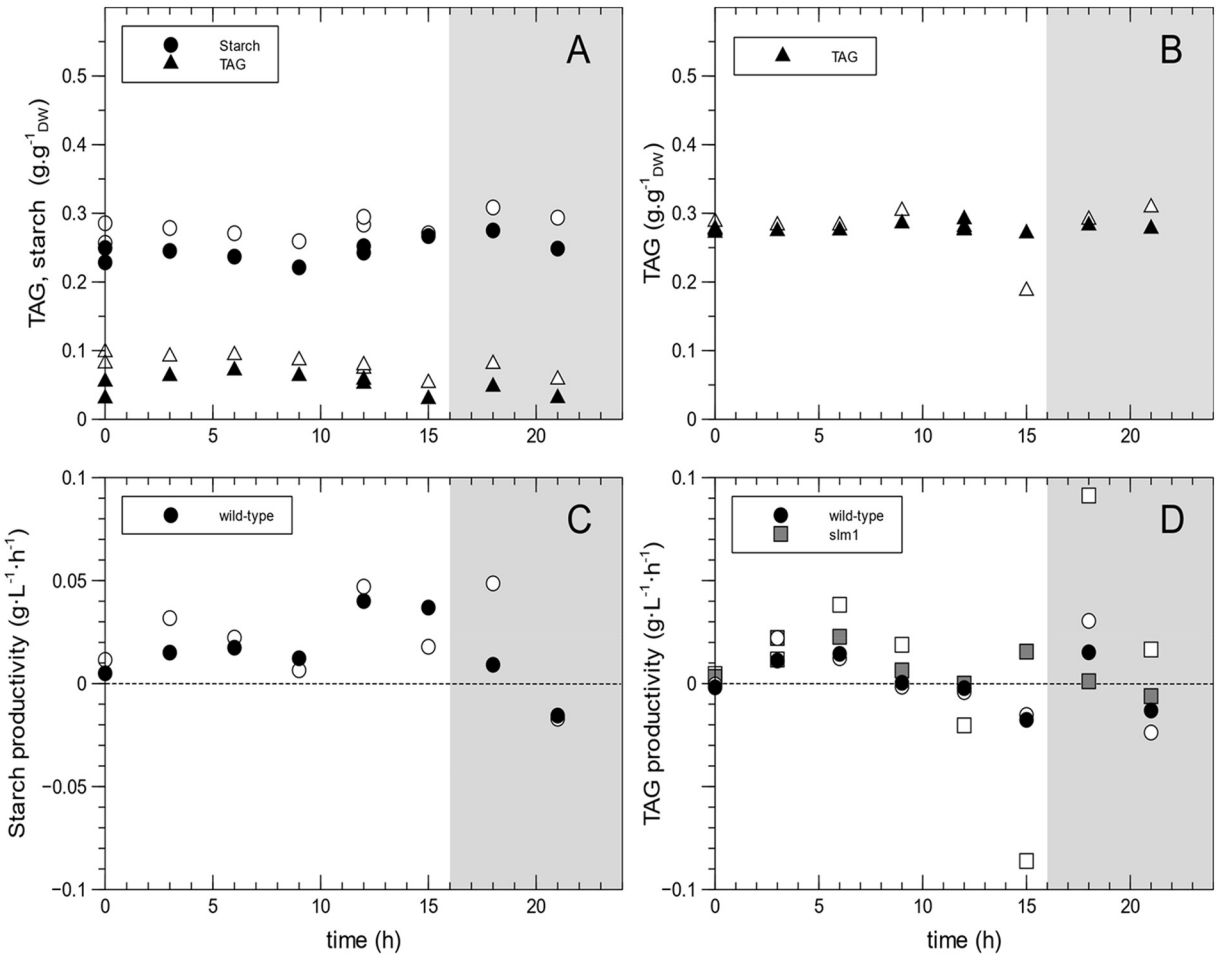

Fig. 2. Diurnal changes under nitrogen limitation in starch and triacylglycerol (TAG) content for *Tetradesmus obliquus* wild-type (A) and slm1 (B) and in starch productivity for the wild-type (C) and TAG productivity for wild-type and slm1 (D). Open and closed symbols represent replicate cultures. The x axis shows hours after the start of the light period. Shaded areas indicate the dark period.

nitrogen limited condition, this maximum content is not reached, which explains the low content of TAG in the wild-type. The preference for starch cannot be explained from the energy density, since more energy can be stored in fatty acids as compared to starch (yield of complete oxidation of fatty acids is about 9 kcal·g^{-1} compared to 4 kcal·g^{-1} for carbohydrates) [28]. A possible explanation for the preference for starch could be that the synthesis and degradation of TAGs requires more cellular resources and enzymes [29]. Another reason might be that when cells grow photoautotrophically, fatty acid synthesis represents a significant loss of carbon as conversion of pyruvate to acetyl-CoA by the pyruvate dehydrogenase complex involves the loss of one of the fixed carbons. This renders starch a more efficient carbon storage compound regarding carbon fixation [30].

For the *slm1* mutant the TAG content (approximately 0.27 g·g$_{DW}$$^{-1}$) was about 4 times higher than for the wild-type during the diurnal cycle (Fig. 2B). However, TAG showed no diurnal oscillations under nitrogen limitation for either strain (Fig. 2A & B). When looking at the TAG productivity, diurnal variations were expected for the *slm1* as the dilution rate is changing. However, no clear diurnal variations were observed (Fig. 2D). This is because the values for dilution rate are similar or smaller than the accumulation term ($\frac{dC_{TAG}}{dt}$). The accumulation term is in turn highly sensitive for small changes in the measured TAG content. Therefore, TAG productivity calculations are highly affected by measurement errors in TAG content. For the wild-type, the values for the dilution rate are higher making the calculation of the TAG productivity less sensitive to small errors in TAG content, which in turn makes the differences between the time points more significant.

The other measured biomass components, proteins and non-starch carbohydrates did not show oscillations through the diurnal cycle for either strain (Supplementary Fig. S1).

3.3. Energy conversion efficiency

Under nitrogen replete conditions, the energy conversion efficiency into biomass of the wild-type is higher than that of the *slm1* mutant [7,13]. We therefore investigated if this was also the case for nitrogen limitation conditions where TAG accumulation occurs. For this, we calculated the minimal number of photons needed for the production of functional biomass, TAG, and starch (for the wild-type), based on the biomass composition of the overflow samples (average steady state values). Results are displayed as a percentage of used photons from the total amount supplied in Fig. 3A. As can be seen, also for nitrogen limited conditions the overall efficiency is lower for the *slm1* mutant than for the wild-type (approximately 50% for the wild-type and 25% for the *slm1*). However, the TAG content of the *slm1* is higher than for the wild-type resulting in a slightly higher TAG volumetric productivity for the *slm1* as compared to the wild-type (0.09 g·L^{-1}·day^{-1} for the wild-type and 0.14 g·L^{-1}·day^{-1} for the *slm1*). The lower overall efficiency is related to the fact that the biomass productivity in the mutant is reduced to less than half of that of the wild-type (1.29 ± 0.11 g·L^{-1}·day^{-1} for the wild-type and 0.52 ± 0.06 g·L^{-1}·day^{-1} for the *slm1*) (Supplementary Table S2). Also, both strains are less efficient under nitrogen limited conditions than under nitrogen replete conditions (62.77 ± 0.08% for the wild-type and 49.75 ± 0.07% for the *slm1*) [13]. When looking into the conversion efficiency during the diurnal cycle in intervals of 1 h (Fig. 3B & C), we observe that during the first half of the day, both strains behave similarly, with the wild-type showing an increase in energy efficiency about 1 h before the *slm1*. However, in the second half of the light period (approximately from t = 7 h), the *slm1* mutant is much less efficient than the wild-type. Notably the second half of the light period is the moment when starch accumulation occurs in the wild-type, probably explaining the extra energy fixed.

Under nitrogen starvation both starch and TAG can act as an overflow sink for electrons [26]. For starchless mutants, it has been suggested that the difference in energy efficiency and biomass yield on light might be due to an increased rate of energy dissipation compared to the wild-type [15,31] since electrons can no longer be channeled to starch. However, under nitrogen limitation growth still occurs and starch still seems to have a role as a diurnal energy storage compound, such as under nitrogen replete conditions [7], which provides an extra benefit for the wild-type compared to the *slm1*.

3.4. Transcriptional landscape

Previous transcriptome analysis on *T. obliquus* under the same LD cycles but in nitrogen replete conditions uncovered that genes following a diurnal expression pattern were contributing to the vast majority of expression changes [12]. Principal component analysis (PCA) of nitrogen replete samples and nitrogen limited samples (this study) under LD cycles, shows that the two first components explain 83% of the total variation in gene expression (Fig. 4A). Samples from both strains (wild-type and *slm1*) grown in the same condition with respect to nitrogen availability and from the same time points overlap. However, the samples taken from the nitrogen replete condition are completely separated from those taken from the nitrogen limited condition. This indicates the limited nitrogen supply has a much greater impact on gene expression than the changes caused by the mutation. In both conditions (nitrogen replete and deplete), there is a clear succession of time points in the PCA. Under nitrogen replete conditions, time points are arranged in a circular pattern (Fig. 4A). However, under nitrogen deplete conditions, the circular pattern seems lost and samples at 3 h overlap with

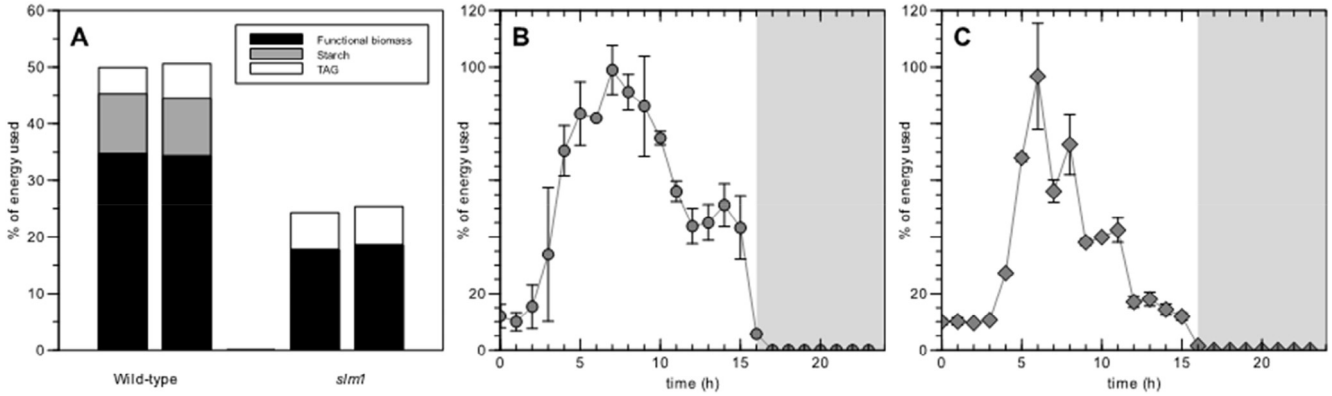

Fig. 3. The percentage of photons (as a fraction of the total supplied) minimally needed to make the different biomass components as an average over 1 day (A) and over each hour of the day for *Tetradesmus obliquus* wild-type (B) and slm1 (C). For (A), values represent the average values of at least 3 overflow samples. For the hourly energy conversion efficiency (B and C) the x axis represents hours after the light was switched on. Values represent average of replicate reactors and error bars represent minimum and maximum values (n = 2). Shaded area indicates the dark period.

the samples at 12 h. Yet, when selecting the genes with a detected diurnal expression, the circular pattern is recovered (Fig. 4B). This noticeable difference was not observed in the nitrogen replete condition, which indicates that nitrogen limitation results in an overall reduction of diurnal changes in expression. The time point samples of each strain in nitrogen limited condition (Fig. 4B) draw an overlapping elliptic pattern, but the variation of expression in *slm1* is clearly lower than in the wild-type. Moreover, the samples of *slm1* during the dark period are all extremely close to each other, indicating very little transcriptional changes. Therefore, starch deficiency has a greater impact on gene expression in nitrogen limited condition than it has in nitrogen replete condition, with *slm1* being particularly inactive during the dark period. In complement, the heatmaps showing similarity of gene expression between time points is available in Supplementary Fig. S3.

3.5. Diurnal gene regulation and functions

Genes with a detected diurnal regulation were clustered using hierarchical clustering based on Pearson's correlation in different numbers of clusters ranging from 3 to 25. Similarities within and differences between clusters were evaluated with well-established indexes, depicted in Supplementary file S4. Based on these results, we considered separating the genes in 5 clusters to be optimal. Similar results are obtained for both strains. The median profile of these 5 clusters is displayed in Fig. 5. Between the two strains, the clusters with the nearest median profile are also the clusters with the most genes in common (Supplementary Fig. S5). For those reasons, clusters were named the same.

As observed in our previous study under nitrogen replete conditions [12], the clusters reflect a succession of peaking expression. Thus, we observe clusters peaking at the night day transition (cluster 1), early day (cluster 2), late day (cluster 3), day night transition (cluster 4) and in the night (cluster 5). Some differences appear in *slm1* expression. Compared to the wild type, expression in the mutant is lower for clusters 1 and 2 (peaking early day) and higher for clusters 4 and 5 (peaking late day and night). For cluster 2 there is also a marked change in profile, as the expression at the end of the day is much lower in the mutant.

The gene clusters of wild-type display a similar succession of transcriptional events as observed in nitrogen replete [12], which consist of protein synthesis, photosystem and pigments synthesis, carbon fixation, cellular replication, glycolysis, cell division, and fatty acid degradation (Table 1). The enrichment analysis revealed differences in amino acid metabolism. Whereas for the wild type processes related to amino acid biosynthesis can be found in all five clusters, for the mutant they are exclusively found in cluster 2 and 3 indicating that amino acid synthesis is restricted to the light period in the mutant. This may be due to the absence of sufficient precursors and energy for amino acid biosynthesis due to the absence of starch in the mutant. In contrast to nitrogen replete conditions [12], under nitrogen limitation both the wild type and mutant show enrichment of genes involved in amino acid degradation during the dark period. Notably, the pathway "Valine, leucine and isoleucine degradation", which produces acetyl-CoA, is found enriched in cluster 5, which is confirmed by the mapping to the metabolic maps (Supplementary file S7). This can be directly explained from the fact that during the night the nitrogen supply is stopped and nitrogen starvation will occur. Amino acid breakdown is then a way to recycle nitrogen to other nitrogen containing compounds. Whereas starch is available in the wild type for energy and precursor generation for the recycling of nitrogen, in the mutant breakdown products of amino acids, like acetyl-CoA can be used for this purpose as exemplified by the enrichment of genes involved in "generation of precursor metabolites and energy" and the increased expression of genes involved in the glyoxylate pathway in the mutant. This pathway converts acetyl-CoA into citric acid cycle intermediates that can be used to synthesize biomass precursors among which new nitrogen containing compounds.

3.6. Selected processes and pathways

Genes associated to carbon fixation, synthesis of the photosystems, its pigments (chlorophylls and carotenoids) and their precursor terpenoid backbone, are all found enriched in the cluster 2 for both strains. Detailed inspection of these pathways (Supplementary file S7) shows all the genes annotated to these consecutive reactions are associated to cluster 2. Also for the nitrogen replete conditions the expression pattern of these genes is the same for both strains and identical to the limiting conditions. This indicates a strong and synchronized regulation of these

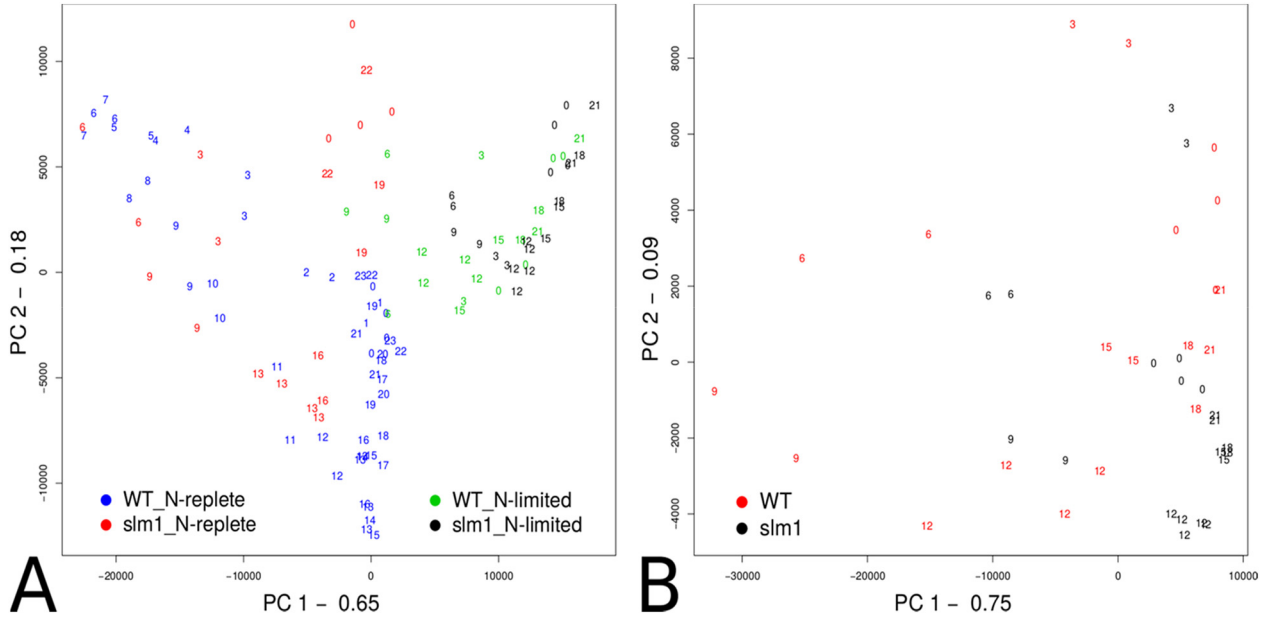

Fig. 4. Principal component analyses of time point samples. (A) Comparison between samples considering all genes (no selection) in nitrogen replete [12] and nitrogen limited conditions. (B) Comparison between samples considering only selected genes (detected time profile) in nitrogen limited conditions. The variance explained by the first two components is indicated on axes labels.

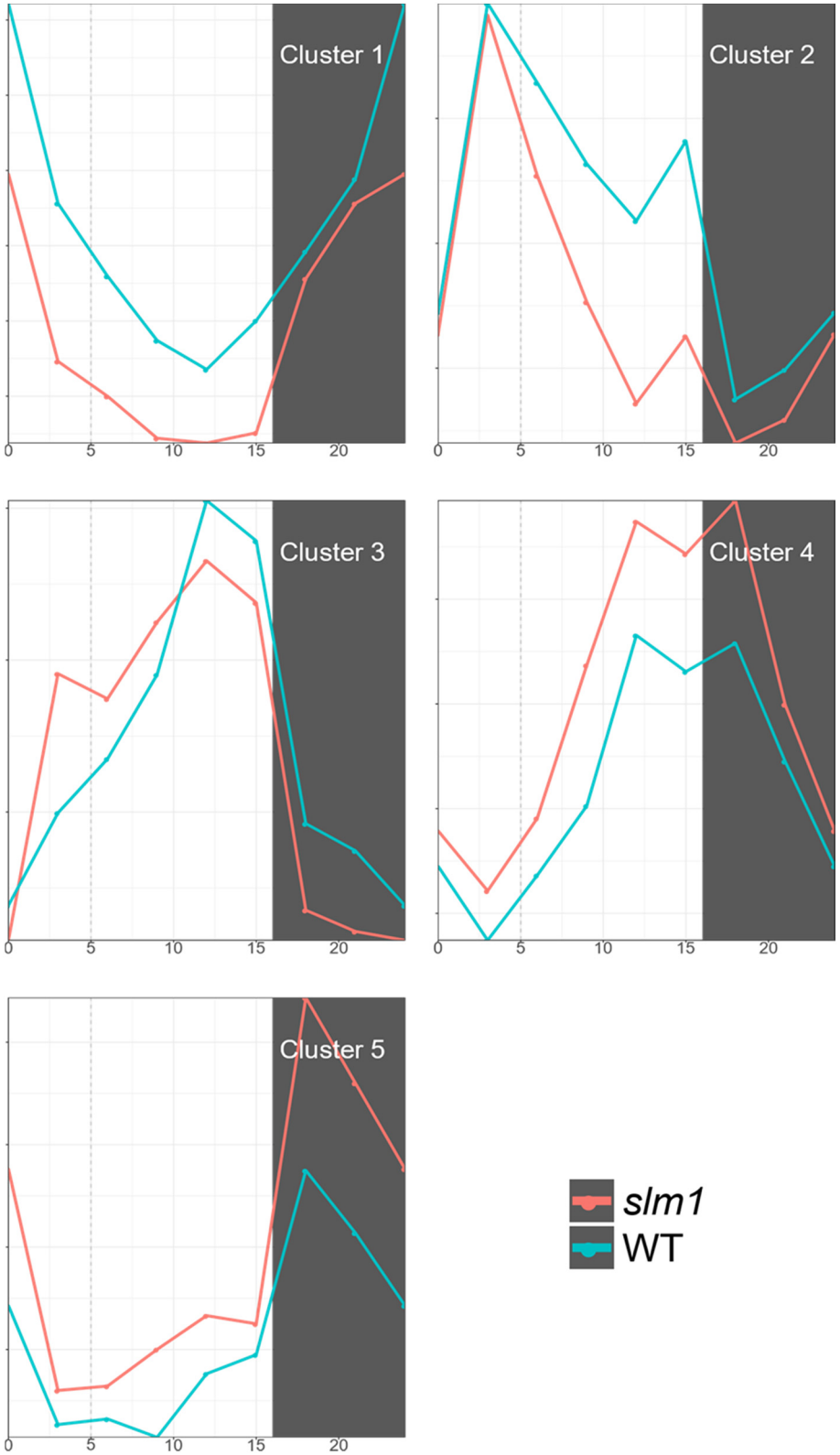

Fig. 5. Expression profile over 16:8 light-dark cycle of the 5 genes clusters identified in both strains. The plots show the median profile of gene expression in the indicated clusters. Dark area represents the dark period.

processes with little to no difference between the strains. We can therefore conclude that these processes are not affected by either the starch deficiency or by the nitrogen limitation. The genes associated to starch synthesis, fatty-acids biosynthesis, carbon fixation, pyruvate metabolism are also tightly regulated within the same time frame. From the detailed pathways overview (Supplementary file S7), we can see that the carbon fixation remains an early process in *slm1*, but the other subsequent pathways and reactions are delayed in comparison to the wild-type strain. These delays reflects the higher difficulty to synthesize the complex machinery required to store energy, due to the nitrogen

Table 1
Results of enrichment analyses. Summary of the results of the enrichment analyses. The first column contains the cluster identifier. The second and third contains the enriched pathways (p-value < 0.0.5). GO terms relate to biological processes (FDR < 0.05) for the wild-type. Fourth and fifth column present the same information for *slm1*. Full set of enrichment results are available in Supplementary file S6.

Cluster	Wild-type		*slm1*	
	Pathway	Biological processes	Pathways	Biological process
1	Fatty acid biosynthesis Glycine, serine and threonine metabolism Starch and sucrose metabolism Pyruvate metabolism Glyoxylate and dicarboxylate metabolism Carbon fixation in photosynthetic organisms	Protein phosphorylation Fatty acid biosynthetic process Oxidation-reduction process	Purine metabolism Geraniol degradation	Protein phosphorylation Movement of cell or subcellular component
2	Ubiquinone and other terpenoid-quinone biosynthesis Photosynthesis Glycine, serine and threonine metabolism Phenylalanine, tyrosine and tryptophan biosynthesis Methane metabolism Carbon fixation in photosynthetic organisms Porphyrin and chlorophyll metabolism Terpenoid backbone biosynthesis Carotenoid biosynthesis Aminoacyl-tRNA biosynthesis	Translation Lysine metabolic process Steroid biosynthetic process Coenzyme metabolic process Aromatic amino acid family metabolic process Photosynthesis Tetrapyrrole metabolic process Dicarboxylic acid metabolic process Cofactor biosynthetic process Oxidation-reduction process Alpha-amino acid biosynthetic process	Glycolysis/gluconeogenesis Fatty acid biosynthesis Ubiquinone and other terpenoid-quinone biosynthesis Pyruvate metabolism Carbon fixation in photosynthetic organisms Porphyrin and chlorophyll metabolism Aminoacyl-tRNA biosynthesis	Cellular amino acid metabolic process Fatty acid metabolic process Photosynthesis Tetrapyrrole metabolic process Pigment metabolic process Carboxylic acid biosynthetic process Cofactor biosynthetic process Oxidation-reduction process Organonitrogen compound biosynthetic process
3	Oxidative phosphorylation Arginine biosynthesis Purine metabolism Pyrimidine metabolism Valine, leucine and isoleucine biosynthesis Lysine biosynthesis Arginine and proline metabolism Histidine metabolism Glutathione metabolism Glyoxylate and dicarboxylate metabolism Aminoacyl-tRNA biosynthesis	RNA methylation tRNA threonylcarbamoyladenosine modification rRNA processing Protein folding Purine ribonucleotide biosynthetic process Purine ribonucleoside triphosphate biosynthetic process Monocarboxylic acid metabolic process Cellular amide metabolic process ATP metabolic process Alpha-amino acid biosynthetic process	Photosynthesis Arginine biosynthesis Purine metabolism Pyrimidine metabolism Alanine, aspartate and glutamate metabolism Lysine biosynthesis	Cellular amino acid biosynthetic process Monocarboxylic acid metabolic process Amide biosynthetic process Nucleobase-containing small molecule metabolic process Oxidation-reduction process
4	Citrate cycle (TCA cycle) Fatty acid biosynthesis Fatty acid elongation Fatty acid degradation Arginine biosynthesis Alanine, aspartate and glutamate metabolism Glycine, serine and threonine metabolism Arginine and proline metabolism Tyrosine metabolism Pyruvate metabolism Propanoate metabolism Butanoate metabolism Carbon fixation pathways in prokaryotes Thiamine metabolism Nitrogen metabolism Drug metabolism - cytochrome P450	Glycolytic process Cellular biogenic amine metabolic process tRNA processing Energy derivation by oxidation of organic compounds	Glycolysis/gluconeogenesis Citrate cycle (TCA cycle) Alanine, aspartate and glutamate metabolism Cysteine and methionine metabolism Glyoxylate and dicarboxylate metabolism Carbon fixation in photosynthetic organisms	

(*continued on next page*)

Table 1 (*continued*)

Cluster	Wild-type		*slm1*	
	Pathway	Biological processes	Pathways	Biological process
5	Glycolysis/gluconeogenesis Galactose metabolism Fatty acid biosynthesis Fatty acid degradation Purine metabolism Pyrimidine metabolism Valine, leucine and isoleucine degradation Phenylalanine metabolism Tryptophan metabolism beta-Alanine metabolism Pyruvate metabolism Propanoate metabolism Methane metabolism	Protein phosphorylation Movement of cell or subcellular component Cell cycle process	Fatty acid biosynthesis Fatty acid elongation Fatty acid degradation Valine, leucine and isoleucine degradation Geraniol degradation Phenylalanine metabolism Tryptophan metabolism Beta-alanine metabolism Alpha-linolenic acid metabolism Pyruvate metabolism Glyoxylate and dicarboxylate metabolism Propanoate metabolism Butanoate metabolism Carbon fixation pathways in prokaryotes Biotin metabolism Biosynthesis of unsaturated fatty acids	Generation of precursor metabolites and energy

limitation and the very limited energy available before light is turned on. Since expression of genes associated to carbon fixation and photosynthesis machinery are not altered unlike what happens to other key systems, we deduce that their role is the most essential, if not critical, and their maintenance is given the highest priority. Possibly, these processes are directly controlled by the light availability. Even if the expression is unchanged, it is possible that the processes are being stretched (or simply delayed) over time by the lack of available nitrogen and starch, effectively delaying the subsequent processes as we observed.

3.6.1. Starch metabolism

As previously observed in two studies [12,32], the lack of starch synthesis in *slm1* is due to a nonsense mutation in the ADP-pyrophosphorylase small subunit. The associated gene was found to be expressed at much lower level in *slm1* than the original gene in wild-type but with a conserved temporal regulation. The reads mapping over the mutant gene revealed the nonsense mutation and more importantly, a homogeneous distribution over the whole gene length. The reduced expression (see Fig. 6) can be explained by a lower transcription or post-transcriptional regulation that would degrade the transcript. Since the diurnal profile of the mutated gene is maintained, it is more likely that the transcript is being degraded instead. Furthermore, the nonsense mutation suggests strongly that this post-transcriptional degradation is done by nonsense-mediated mRNA decay (NMD) [33,34]. Since this quality-control mechanism is common in eukaryotes, it is very likely that *Tetradesmus obliquus*, and possibly other green algae are subjected to NMD. Nevertheless, it should be noted that *slm1* has been obtained with UV therefore we cannot rule out other mutations that could affect regulation.

As previously observed in nitrogen replete condition, the similarity of expression between the two strains means that there is little response from the lack of starch. The strongest observed difference is for the gene g2865.t1, annotated to the starch synthase (EC 2.4.1.21, Fig. 6). Its expression is effectively doubled in the *slm1* as compare to in the wild-type. Another noticeable difference relates to gene g234.t1, associated to the starch branching enzyme (EC 2.4.1.18). This gene is over-expressed in *slm1*, but with a very similar time profile to that in wild-type (Fig. 6). Though the starch synthesis is operated by few enzymes, we did not observe a strong response in the mutant that could be attributed to a transcription regulatory mechanism to counter the incapacity to synthesize ADP-Glucose and starch. Since the transcript g2865.t1 coding for the starch synthase (EC 2.4.1.21) is the only one that displays a change in diurnal expression profile, it is likely to be a regulatory point for synthesizing starch in the microalga *T. obliquus*. Furthermore, the same transcript had also different expression between strains in nitrogen replete condition. Unlike here, the change in nitrogen replete was an early shift in expression [12]. However, we cannot rule out other post-translational regulatory mechanisms.

Similarly to starch synthesis, the expression of genes associated to starch degradation does not seem to be affected by the incapacity to synthesize starch. We identified genes associated to five enzymatic reactions. The profiles of these genes are shown in Fig. 7 except for the glucoamylase (EC 3.2.1.3) which did not have a detected time profile. Isoamylase (EC 3.2.1.68) was found in the same cluster for both strains and showed identical profiles for both associated genes (Fig. 7). The alpha-amylase (EC 3.2.1.1) has several candidate genes, but significant changes were observed only for g17712.t1. This gene was found in wild-type cluster 4 and in *slm1* cluster 3, with an apparent higher expression during the light period and lower expression during the dark period. As for the beta-amylase (EC 3.2.1.2), the associated gene (g13560.t1) displays a significant difference between the two strains, with a generally higher expression and a strong peak right after the switch to dark at 18 h (Fig. 7) for *sml1*. Finally, the glycogen phosphorylase (EC 2.4.1.1) was associated to two genes and both were affected in a similar way, since they were found in wild-type cluster 4 and in *slm1* cluster 3. While the beta-amylase and the isoamylase are more expressed during the dark period, the alpha-amylase and the glycogen phosphorylase are more expressed at the end of the light period. The first two are degrading beta glycosidic linkage, while the latter two are degrading alpha glycosidic linkage. The latter two are also displaying a stronger decrease right after dark in *slm1*. These results suggest that the genes associated to alpha and beta linkage lysis are not only expressed differently over time, but are also regulated differently by starch deficiency.

Overall, the expression of the genes associated to the starch synthesis and degradation agrees with the biochemical measurements. For the wild type, the genes associated to starch synthesis show diurnal regulation with higher expression during the first half of the light period, which agrees with the accumulation of starch later on. Likewise, the genes involved in degradation are upregulated either just before or during the dark period, which agrees with the observed starch degradation. With respect to *slm1*, the genes associated to the starch synthesis are strongly upregulated during the day, which may be a

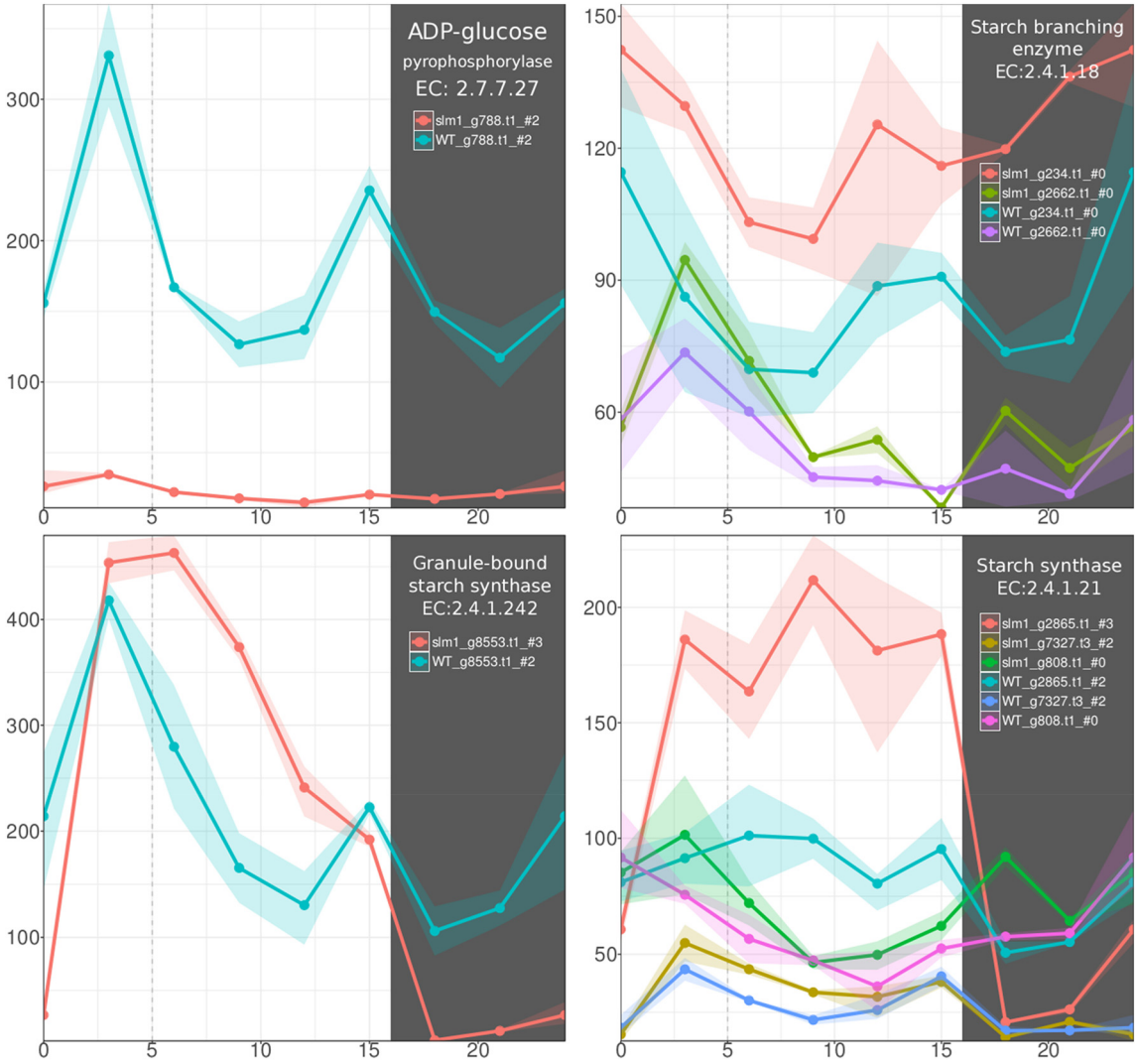

Fig. 6. Diurnal expression of genes associated to starch synthesis. Points represent mean values for each time point (n = 2), the ribbon covers the minimum and maximum values for each time points. The genes associated to the same EC number are plotted together with the same scale Each plot is labeled with the reaction name, the corresponding EC number, and the color legend for each gene-strain combination. For each gene-strain combination, the number after the # symbol, indicates the associated cluster and #0 indicates that the gene showed not significant changes in expression over time. The dark area corresponds to the dark period.

physiological response to the inability to shuttle an excess of energy and carbon to starch. Likewise, a few of the degradation enzymes are up regulated during late light period or during the dark period, which may be again, a response to the lack of transient energy due to the absence of starch.

3.6.2. Metabolism of lipids and TAGs

The wild-type expression of genes associated to lipid synthesis fits a general trend: highest expression is reached right at the beginning of the light period, lowest expression is reached half way of the light period, increase of expression right before the dark period, and slight decrease during the dark period (Fig. 8). This trend is very similar to the TAG productivity measured in Fig. 2D, and the first peak corresponds to the increased TAG productivity at 6 h (Fig. 2), but with a short delay. Remarkably, the same genes in *slm1* display larger variations in expression with the lowest expression during the dark and highest expression during the day. The increased expression at the peaks is roughly 1.5 to 2 times higher in *slm1* than in the wild-type. This difference suggests that the lack of the ability to synthesize starch is actively compensated by increased accumulation of lipids and TAG during the light period. Furthermore, the presence of starch correlates with a maintained expression of the lipid synthesis enzymes during the night, whereas in the absence of starch these enzymes are no longer expressed in the night. This suggests that starch is possibly used to synthesize lipids and TAG when there is no photosynthesis.

3.6.2.1. TAG and lipid synthesis

In the pyruvate metabolism, pyruvate dehydrogenase subunits synthesizing acetyl-CoA (EC 1.2.4.1, 2.3.1.12, 1.8.1.4) appear in wild-type cluster 1 and *slm1* cluster 2 (Supplementary file S7), which could be related to the fact that *slm1* cannot synthesize acetyl-CoA from starch during the dark because starch is not present. Acetyl-CoA is involved in many processes, but most importantly, it is the building block to start the lipid synthesis by the Acetyl-CoA carboxylase (ACC, EC 6.4.1.2). As seen in Fig. 8, the best candidate genes for the ACC are all found in wild-type cluster 1 and *slm1* cluster 2 and 3. All these time profiles are very similar to each other, which is synchronized with the described synthesis of acetyl-CoA. The following reaction in the lipids synthesis is the Beta-ketoacyl-ACP synthase I (KASI, EC 2.3.1.41). Two genes were associated to this reaction, g16858.t1 and g14707.t1, where g16858.t1 is identified with a trans-membrane domain and g14707.t1 is not. The two genes are expressed with near identical profiles fitting into wild-type cluster 1 and *slm1* cluster 2. Overall, the same pattern is observed for genes associated to reactions in the lipids biosynthesis

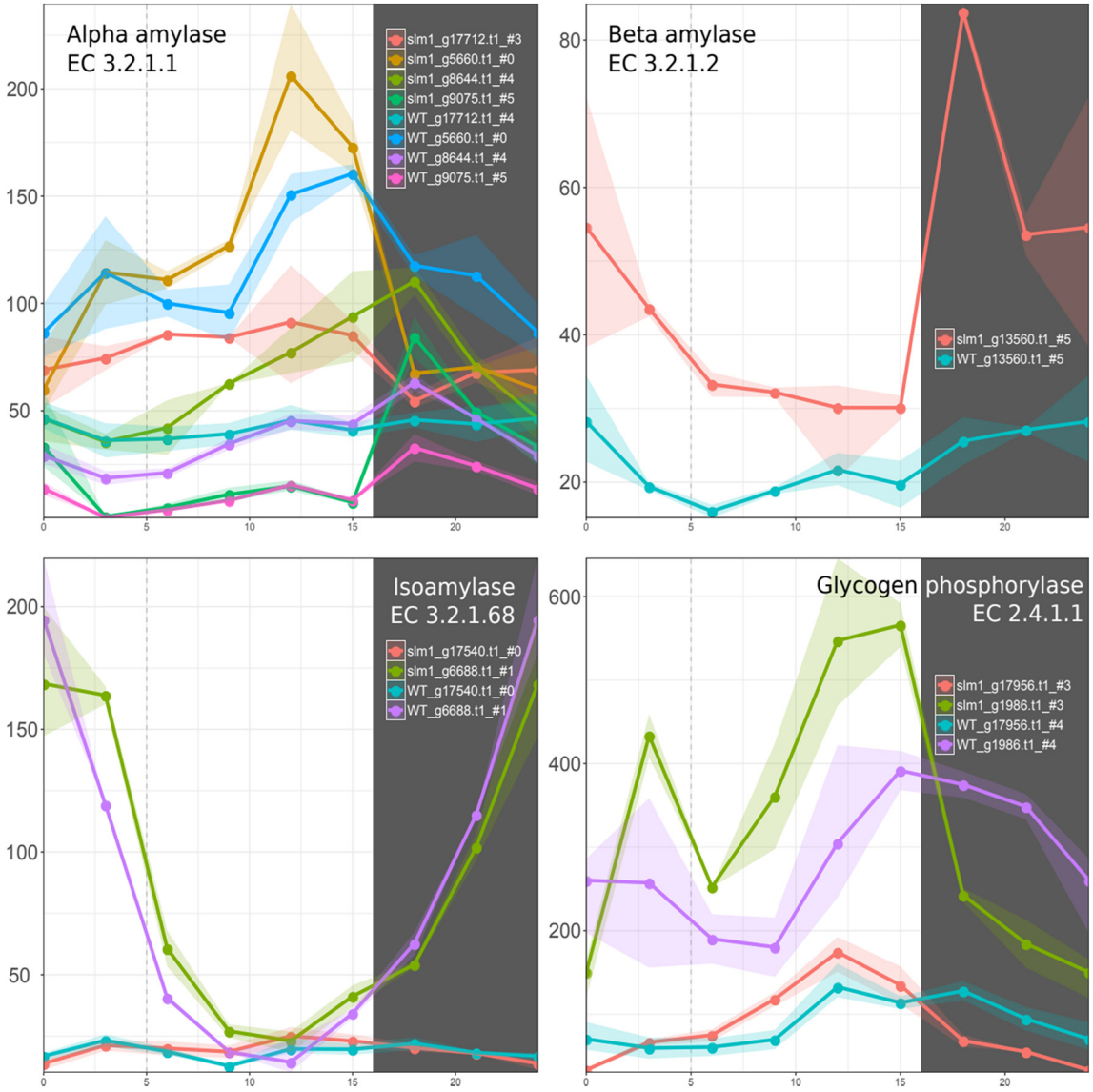

Fig. 7. Diurnal expression of genes associated to starch degradation. Points represent mean values for each time point (n = 2), the ribbon covers the minimum and maximum values for each time points. The genes associated to the same EC number are plotted together with the same scale Each plot is labeled with the reaction name, the corresponding EC number, and the color legend for each gene-strain combinations. For each gene-strain combination, the number after the # symbol, indicates the associated cluster and #0 indicates that the gene showed not significant changes in expression over time. The dark area corresponds to the dark period.

(Supplementary Fig. S8). The Acyl-CoA synthetase (EC 6.2.1.3) is associated to two genes, displaying very different patterns. This is because it is a reversible reaction that is occurring also in the beta oxidation pathway. Our results and the manual curation of the annotation confirm that g1817.t1 performs the forward reaction, towards synthesis, while g4377.t1 performs the reverse reaction. The forward reaction is in phase with the other synthesizing genes.

The synthesis of TAG can be performed by two different enzymatic reactions, known as diacylglyceride acyltransferase (DGAT, EC 2.3.1.20) and phospholipid diacylglycerol acyltransferase (PDAT, EC 2.3.1.158). While several DGAT genes have been identified in green algae, our functional annotation revealed two genes with high confidence [35]. The expression of these two genes is noticeably different, with g8527 being the only one with a temporal regulation. In wild-type, the gene g8527 is highly expressed during the dark period. In *slm1*, its profile is very similar to the wild-type but with overall higher expression and apparently more exclusive to the dark period. In *slm1*, PDAT is displaying a somewhat opposite expression to DGAT, meaning that fatty acids from phospholipids are transferred onto diacylglycerides (DAG) to form TAG during the light period and free fatty acids are added to DAG during the dark period. This seems to agree with the findings in *Chlamydomonas reinhardtii*, where PDAT mediated membrane lipid turnover is helping to recycle phospholipids and synthesize TAG [36]. Interestingly, the monogalactosyldiacylglycerol (MGDG) synthase (EC 2.4.1.46) is highly expressed during the light period with a similar pattern in both strains. This expression is not synchronized with any of the other lipids synthesis reactions, but because MGDG is the main lipid form of the chloroplast membrane, the expression of the MGDG synthase is logically correlated with cellular growth and chlorophyll synthesis.

3.6.2.2. TAG and lipid degradation. In the wild-type strain, the diurnal expression of genes associated to TAG and lipid degradation shows a temporal regulation very similar to that of genes associated to synthesis, but with a lower expression. These genes are expressed higher during the day period and lowest at night. This transcriptional regulation is coherent with the measured accumulation of TAG and lipids during the day and night, and with a very limited turnover.

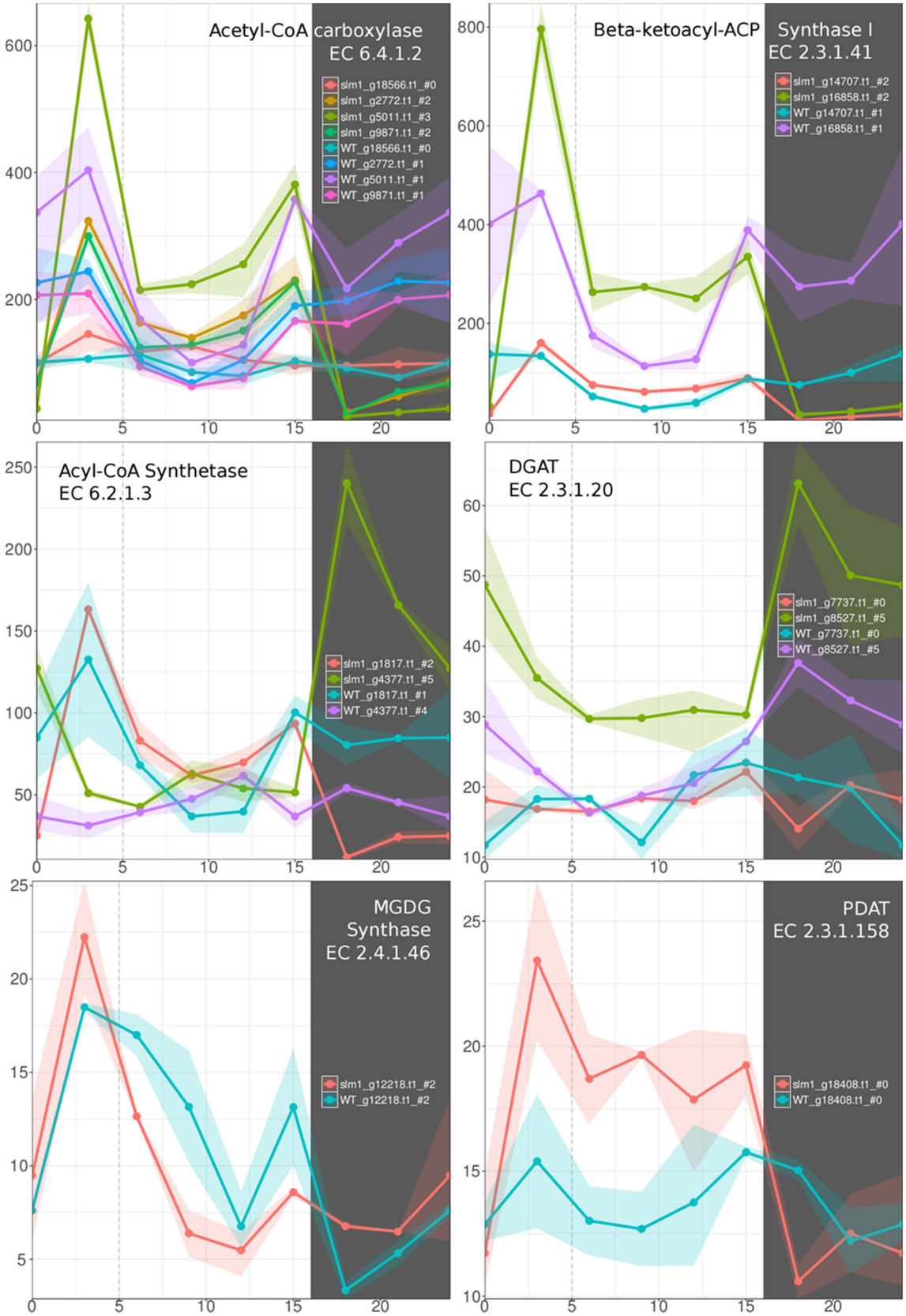

Fig. 8. Diurnal expression of genes associated to lipid and TAG synthesis. Points represent mean values for each time point (n = 2), the ribbon covers the minimum and maximum values for each time points. The genes associated to the same EC number are plotted together with the same scale. Each plot is labeled with the reaction name, the corresponding EC number, and the color legend for each gene-strain combination. For each gene-strain combination, the number after the # symbol, indicates the associated cluster and #0 indicates that the gene showed not significant changes in expression over time. The dark area corresponds to the dark period.

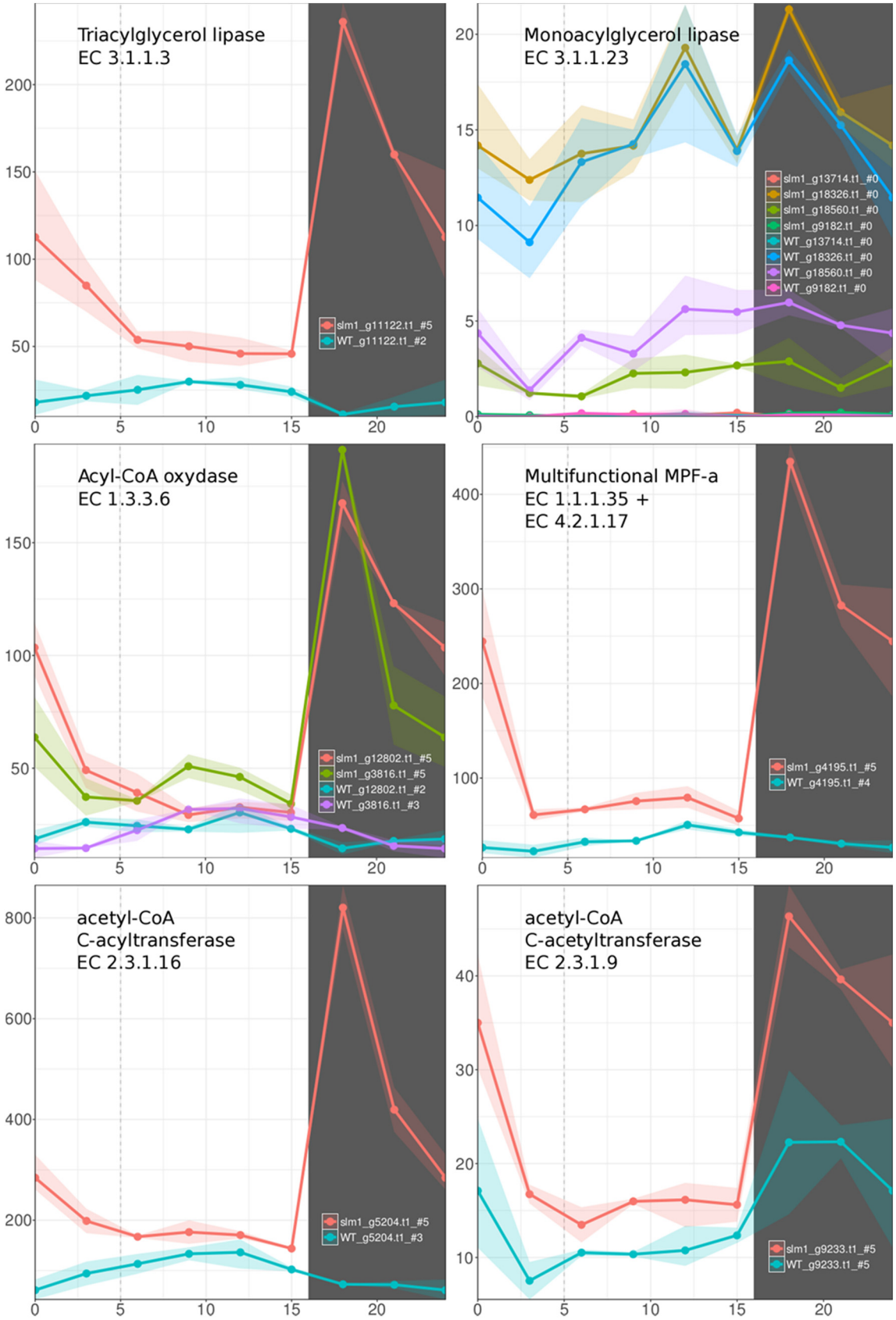

Fig. 9. Diurnal expression of genes associated to lipid and TAG degradation. Points represent mean values for each time point (n = 2), the ribbon covers the minimum and maximum values for each time points. The genes associated to the same EC number are plotted together on the same scale. Each plot is labeled with the reaction name, the corresponding EC number, and the color legend for each gene-strain combination. For each gene-strain combination, the number after the # symbol, indicates the associated cluster and #0 indicates that the gene showed not significant changes in expression over time. The dark area corresponds to the dark period.

However, the *slm1* strain is regulated in a complete opposite way, strongly over-expressing the genes associated to TAG and lipid degradation during the dark period (Fig. 9). Though the profile of *slm1* under N-limitation is very similar to that in the previously analyzed replete condition [12], the amplitude of the up-regulation at dark is much more important, with fold changes ranging from 1.5 to 2.5 folds. Interestingly, also the acyl-CoA oxidase (EC 1.3.3.6) is now displaying a strong increase in expression in *slm1* compared to the wild-type.

The first and second step to degrade TAG is performed by the same enzyme, the triacylglycerol lipase (EC 3.1.1.3). Its highest expression is measured at 18 h, the first time point after dark, and its expression reduces progressively until 6 h (Fig. 9). Next, the last fatty acid chain is removed from the glycerol by the monoacylglycerol lipase (EC 3.1.1.23). Out of the four genes annotated to this reaction, only two displayed some expression variation, although these appear lowly expressed and do not display any temporal regulation (Fig. 9). The following step is the Acyl-CoA synthetase, the reversible reaction described in the synthesis section (Fig. 8), for which we have identified separate candidates proteins for each direction. The degrading candidate (g4377.t1) is highly expressed during the dark period, which is in phase with the other degrading candidates. The four following reactions are repeated reactions and are performed by three enzymes: Acyl-CoA oxydase (EC 1.3.3.6), Multifunctional MPF-a (EC 1.1.1.35, 4.2.1.17), Acetyl-CoA acyltransferase (EC 2.3.1.16), Acetyl-CoA *C*-acetyltransferase (EC 2.3.1.9). All the reactions are highly expressed in *slm1* during the dark period. Only the Acetyl-CoA *C*-acetyltransferase is expressed with a similar time profile in the wild-type strain but at a lower level. Additionally, the enzyme representing the beta oxidation of unsaturated fatty-acids, enoyl-CoA isomerase (EC 5.3.3.8), is found to be expressed in the same cluster as the other degrading enzymes (*sml1* cluster 5, Supplementary file S7).

The acetyl-CoA molecules produced from the described reactions can then be utilized by the organism. For example, the acetyl-CoA can be broken down in the TCA cycle to generate energy or can be converted into succinate and malate through the glyoxylate cycle. Next succinate and malate can be converted into oxaloacetate through the TCA cycle in the mitochondria, and finally converted into hexoses or sucrose through the glyconeogenesis in the cytosol [37]. Overall, all these points strongly suggest that a global regulatory mechanism, as observed in *A. thaliana* [38], allows the organism to use TAG as a form of transient energy storage, which accumulates during the light period and is degraded during the dark period.

3.6.3. Nitrogen metabolism

The expression profiles of the genes associated to nitrogen metabolism are displayed in Fig. 10. Very little difference is noticeable between the strains at the first sight as most of the profiles are overlapping and only one gene stands out. Five genes from three of the six annotated reactions are in cluster 4, resulting in an enrichment of this pathway. These strong similarities suggest that nitrogen metabolism in both strains is regulated in a very similar way. In other words, nitrogen metabolism is mostly affected by nitrogen limitation and not from starch availability.

In the previous paper on N-replete conditions we could not find a protein for nitrate reductase. In this work we were able to identify a candidate protein for nitrate reductase [12]. The EnzDP score for this protein came second. However, its expression is sufficient, unlike the top scored protein that was not found expressed in both the nitrogen limited condition as well as the nitrogen replete condition. Both strains display the exact same pattern and level of expression for this protein, fitting the associated cluster 4 pattern but with only the peak of expression before the dark period (Fig. 10). This diurnal expression pattern indicates that for the wild type and *slm1* under nitrogen limitation, nitrogen is assimilated gradually throughout the whole light period and gradually reduced right before the dark period until the very early light period. In the nitrogen replete condition, the expression of the transcript for sml1 is identical to the one observed here in the nitrogen limited condition, and is part of the *slm1* cluster A as defined in the previous N-replete paper [12]. Besides, the wild-type expression is very different and fits the pattern of cluster 5 as defined in the N replete paper [12], with a progressive expression throughout the light period similar to the *slm1* pattern in this study, but with a continued high expression during the late day and early night, where the expression of the *slm1* dropped. Its expression reached its highest value early in the dark period after which it decreased. This seems to indicate that nitrogen is probably metabolized during the dark period. Since this reaction requires the presence of nitrogen and energy in form of NADH, it can only occur in nitrogen replete conditions for strains with available transient energy storage like starch.

The genes associated to the nitrite reductase and the nitrite reductase NO-forming are too lowly expressed to detect any time pattern. Hence, it is unlikely that these are used by *Tetradesmus obliquus* to perform the reduction of nitrite. Besides, two genes were associated to two forms of hydroxylamine reductase (EC 1.7.99.1, Fig. 10). These two are expressed differently throughout the diurnal cycle, their expression is not affected by the mutation of *slm1*, and the expression of the hybrid cluster protein (HCP) is much higher (~10 folds). More interestingly, the diurnal expression of the transcript associated to the HCP is nearly identical to the one observed from the nitrate reductase. In addition, the same expression is also observed between the two transcripts in nitrogen replete condition. Since the gene identifiers are given by their order of appearance in the genome, it is clear that the nitrate reductase and the HCP are neighbor genes, further indicating that these genes have a special bound. Additionally, the hydroxylamine reductase reaction is fairly similar to the nitrite reductase and was even found to perform the NO forming nitrite reduction [39]. We are pushed to believe that the proteins translated from these transcripts (g618.t1 and g619.t1), though different than known enzymes, are performing the successive reactions of nitrate and nitrite reduction. It would then be valuable to confirm the functionally of these two proteins.

The glutamine synthetase (GS, EC 6.3.1.2, g10416.t1) is highly expressed throughout the whole light period, and lowly expressed during the dark period, effectively fitting clusters 2 and 3 of wild-type and *slm1* respectively. In both strains the expression is very similar. Compared to our previous observations in nitrogen replete conditions, its maximum expression in nitrogen limiting conditions is about 3 times lower and its expression profile is very different. In the nitrogen limited condition, its expression is high throughout the whole light period, while in nitrogen replete, its expression was high during the early light period and the dark period. Among the glutamate synthase (GltS, EC 1.4.1.14) in nitrogen replete condition, only the ferredoxin-dependent glutamate synthase (fd-GltS) was displaying significant differences between the strains and it was down-regulated in *slm1*. However, in this nitrogen limited condition, fd-GltS only displays a marginal difference at 3 h between the strains with a slight overexpression. The levels of expression are comparable to *slm1* in nitrogen replete condition. Most importantly, while the two NADH dependent GltS are displaying a similar profile between strains, their expression is roughly 2 folds higher in *slm1* than in the wild-type. Overall, it appears that when *T. obliquus* is exposed to nitrogen limitation, it relies more on the NADH dependent GltS than the fd-GltS, and with an even stronger expression for *slm1*. It would seem that with increasing stress, GltS is more prominent over fd-GltS, possibly due to stopped ferredoxin oxidation by the photosystem I.

Green algae are known to synthesize glutamate with GS, GltS, and fd-GltS, while ammonia is recycled by the glutamate dehydrogenase (GDH, EC 1.4.1.3) from metabolites such as amino acids [40]. Deamination by GDH suggests that amino acids are used as source of energy and possible ammonium for protein recycling during the heterotrophic condition present in the dark period. Proteins are recycled for different purposes: to regulate enzyme activities, to remove abnormal proteins, to generate energy and to adapt to the changing environment [41].

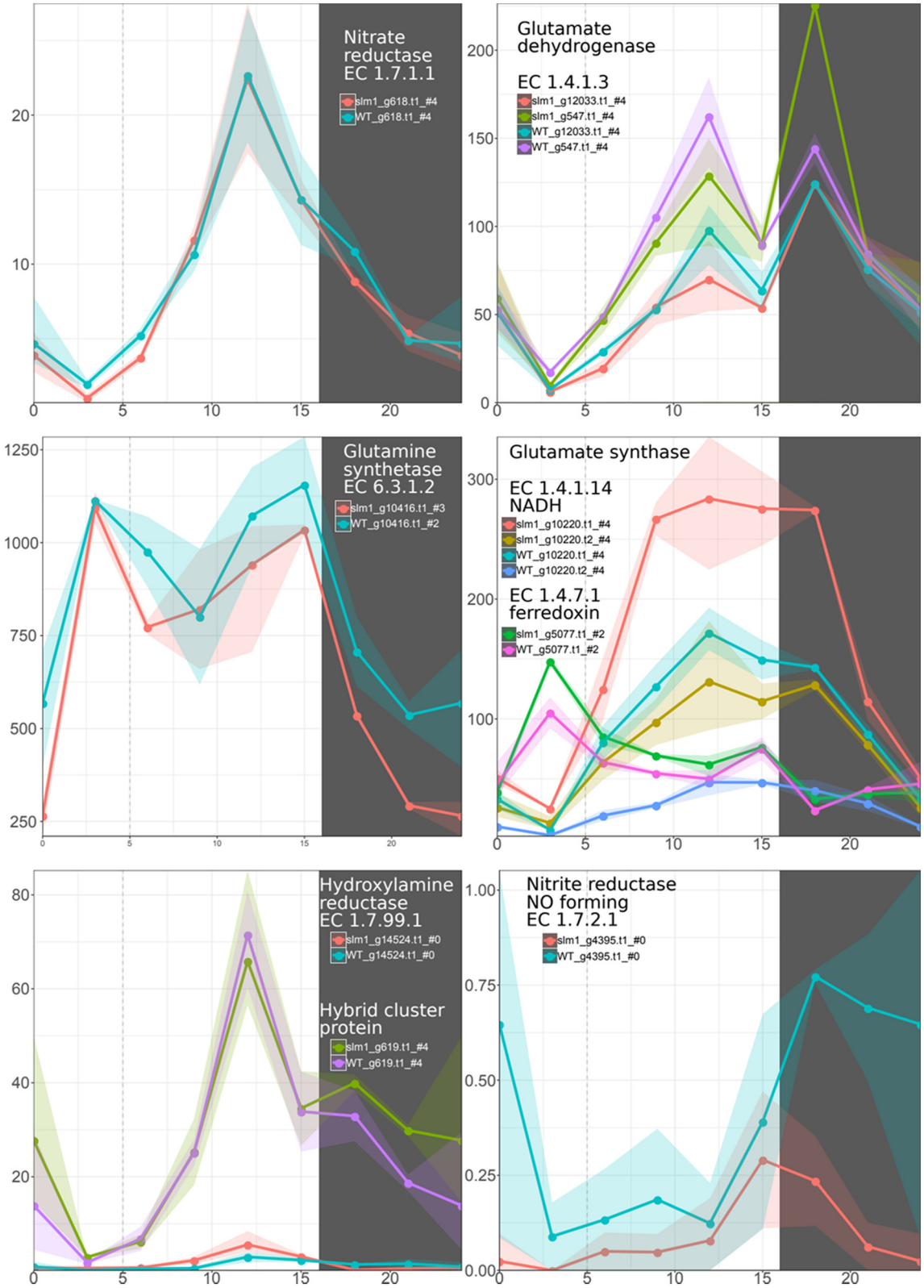

Fig. 10. Diurnal expression of genes associated to nitrogen metabolism. Points represent mean values for each time point (n = 2), the ribbon covers the minimum and maximum values for each time points. The genes associated to the same EC number are plotted together on the same scale. Each plot is labeled with the reaction name, the corresponding EC number, and the color legend for each gene-strain combination. For each gene-strain combination, the number after the # symbol, indicates the associated cluster and #0 indicates that the gene showed not significant changes in expression over time. The dark area corresponds to the dark period.

Protein turnover is believed to be an adaptive process and also to be one of the most energy demanding processes during dark respiration [42–44]. Similarly to our previous findings in nitrogen replete conditions, among the genes associated to GDH, only g547.t1 displays a difference between the strains with for *slm1* a lower peak of expression just before dark and a higher peak of expression just after the start of

the dark period. Even if the difference between the strains is not large and the peak before dark has overlapping values, the values in the second peak are significantly different. In fact, the replicate values are much closer to each other, and the minimum difference between the strains is ~1.5 folds higher for *slm1*. More subtly, after being subjected to nitrogen limitation, only *slm1* kept the high peak of expression after dark. The stronger GDH activity, the enrichments for "generation of precursor metabolites and energy", enrichment for diverse amino acids pathways (including degrading ones), transaminases candidate proteins, and other enzymes involved in the amino acids degradation, indicate that amino acids are actively degraded at the end of the light period and during the dark period, with higher *slm1* activity in the dark period.

3.6.4. Glyoxylate cycle

The "Glyoxylate and dicarboxylate metabolism" that is enriched in wild-type cluster 1 and 3, and is enriched in *slm1* cluster 4 and 5. The glyoxylate pathway converts Acetyl-CoA, which is a breakdown product of amino acids, fatty acids and nucleic acids, to compounds containing 4 carbon atoms like succinate, fumarate, malate and oxaloacetate. These C4 compounds in turn can then be converted to building blocks for biomass components. This is a sign that components from degradation pathways are recycled to new biomass components for example for remodeling the protein and fatty acid composition of the cell. In the previous sections we have shown that the gene expression data during the dark period display clear signs of degradation of amino-acids, fatty-acids and TAG for *slm1*. However, looking at the biochemical measurements for *slm1*, degradation during the dark period cannot be observed (Fig. 2, Supplementary Fig. 1).

The glyoxylate cycle converts two acetyl-coA molecules to one malate molecule and contains two specific enzymes that are not found in the TCA cycle. The transcripts associated to these key enzymes, cycle malate synthase (MS, g18100.t1) and isocitrate lyase (ICL, g13192.t1), are both found in wild-type cluster 3, while for *slm1* they are in cluster 5. Their expression profile in *slm1* is identical to the lipid degrading enzymes (I.g. ACC, Fig. 9), and most importantly, orders of magnitude higher than the wild-type. We have also analyzed the other reactions involved in the glyoxylate cycle, and we have identified candidate proteins that agree with *slm1* dark period activity (Supplementary file S9). These results suggest that the glyoxylate cycle is only active in *slm1* and exclusively during the dark period. This confirms that in *slm1* fatty acids are broken down to acetyl-CoA to directly generate energy from. At the same time the glyoxylate pathway is used to convert acetyl-CoA to intermediates of the TCA cycle to keep this cycle running, or use them to make various biomass components. Finally also some amino acids are broken down to glyoxylate or acetyl-CoA and can be used in this way.

4. Conclusions

Under continuous nitrogen limitation, both *T. obliquus* wild-type and *slm1* showed a repeated diurnal dilution pattern, with the *slm1* showing a lower 24 h dilution rate (growth rate) compared to the wild-type. The transcriptome analysis revealed a similar diurnal pattern, with a reduced amplitude of the changes in expression for *slm1*. Under nitrogen limitation, *T. obliquus* wild-type continued to prefer starch to store energy and carbon. Starch was accumulated to an average content of approximately $0.25\ g{\cdot}g_{DW}{}^{-1}$. Additionally, starch showed small diurnal oscillations, confirming its role as a transient energy storage compound, but to a lower extent than under nitrogen replete conditions. Analysis of expression changes during the cycle of genes associated to starch synthesis and degradation correlate with the measured productivity. The possibility to synthesize starch provides an advantage for the wild-type as compared to *slm1* as it has a higher energy conversion efficiency into the biomass components. With respect to the diurnal cycle this higher efficiency of the wild-type is reached especially during the last hours of light, where starch is accumulated. The energy conversion efficiency of photons into biomass components for the *slm1* was only half of the one obtained for the wild-type, which resulted in a decrease in biomass productivity in *slm1* (from $1.29\ g_{DW}{\cdot}L^{-1}{\cdot}day^{-1}$ for the wild-type to $0.52\ g_{DW}{\cdot}L^{-1}{\cdot}day^{-1}$ for the *slm1*). However, the TAG content in the *slm1* was higher than for the wild-type (average steady state values of approximately $0.27\ g{\cdot}g_{DW}{}^{-1}$ for *slm1* compared to $0.07\ g{\cdot}g_{DW}{}^{-1}$ for the wild-type), which resulted in a slightly higher TAG volumetric productivity for the *slm1* as compared to the wild-type ($0.09\ g{\cdot}L^{-1}{\cdot}day^{-1}$ for the wild-type and $0.14\ g{\cdot}L^{-1}{\cdot}day^{-1}$ for the *slm1*).

The transcriptome analysis revealed breakdown of lipids and proteins in *slm1* during the dark period, which are probably used for the generation of energy in the absence of starch. In agreement with this, the enzymes in the glyoxylate cycle are upregulated in the *slm1* mutant. This cycle is used to convert the acetyl-CoA from amino acid and fatty acid breakdown to intermediates of the citric acid cycle to either keep this cycle running or to be converted to other biomass components. Our measurements do not show significant diurnal variation in DW proteins and TAG content, which indicates that substantially less energy is generated in the mutant during the dark period.

Supplementary data to this article can be found online at https://doi.org/10.1016/j.algal.2020.101937.

Funding

This research project was supported by the Consejo Nacional de Ciencia y Tecnología – CONACYT, Mexico, Scholar 218586/Scholarship 314173. In addition, GMLS is part of the program "Doctores Jóvenes para el Desarrollo Estratégico Institucional" by the Universidad Autónoma de Sinaloa. This work has been financially supported by the Systems Biology Investment Program of Wageningen University (KB-17-003.02-29).

CRediT authorship contribution statement

G. Mitsue León-Saiki: Conceptualization, Methodology, Investigation, Formal analysis, Writing - original draft, Visualization. **Benoit M. Carreres:** Conceptualization, Methodology, Software, Formal analysis, Data curation, Writing - original draft, Visualization. **Ilse M. Remmers:** Conceptualization, Methodology, Investigation, Writing - review & editing. **René H. Wijffels:** Conceptualization, Writing - review & editing, Supervision, Funding acquisition. **Vitor A.P. Martins dos Santos:** Conceptualization, Writing - review & editing, Supervision, Funding acquisition. **Douwe van der Veen:** Conceptualization, Methodology, Formal analysis, Writing - review & editing, Supervision. **Peter J. Schaap:** Conceptualization, Methodology, Formal analysis, Writing - review & editing, Supervision. **Maria Suarez-Diez:** Conceptualization, Methodology, Formal analysis, Data curation, Writing - review & editing, Supervision. **Dirk E. Martens:** Conceptualization, Methodology, Formal analysis, Writing - review & editing, Supervision.

Declaration of competing interest

The authors declare that they have no known competing financial interests or personal relationships that could have appeared to influence the work reported in this paper.

Acknowledgments

The authors would like to thank Tom Schonewille for the RNA extraction of all samples.

Statement of informed consent, human/animal rights

No conflicts, informed consent, or human or animal rights are applicable to this study.

References

[1] Y. Chisti, Constraints to commercialization of algal fuels, J. Biotechnol. 167 (2013) 201–214.
[2] A.J. Klok, P.P. Lamers, D.E. Martens, R.B. Draaisma, R.H. Wijffels, Edible oils from microalgae: insights in TAG accumulation, Trends Biotechnol. 32 (2014) 521–528.
[3] R.H. Wijffels, M.J. Barbosa, M.H.M. Eppink, Microalgae for the production of bulk chemicals and biofuels, Biofuels Bioprod. Biorefin. 4 (2010) 287–295.
[4] L. de Winter, A.J. Klok, M. Cuaresma Franco, M.J. Barbosa, R.H. Wijffels, The synchronized cell cycle of Neochloris oleoabundans and its influence on biomass composition under constant light conditions, Algal Res. 2 (2013) 313–320.
[5] L. Krienitz, C. Bock, Present state of the systematics of planktonic coccoid green algae of inland waters, Hydrobiologia 698 (2012) 295–326.
[6] G. Breuer, P.P. Lamers, D.E. Martens, R.B. Draaisma, R.H. Wijffels, Effect of light intensity, pH, and temperature on triacylglycerol (TAG) accumulation induced by nitrogen starvation in Scenedesmus obliquus, Bioresour. Technol. 143 (2013) 1–9.
[7] G.M. León-Saiki, I.M. Remmers, D.E. Martens, P.P. Lamers, R.H. Wijffels, D. van der Veen, The role of starch as transient energy buffer in synchronized microalgal growth in Acutodesmus obliquus, Algal Res. 25 (2017) 160–167.
[8] S.H. Ho, C.Y. Chen, J.S. Chang, Effect of light intensity and nitrogen starvation on CO2fixation and lipid/carbohydrate production of an indigenous microalga Scenedesmus obliquus CNW-N, Bioresour. Technol. 113 (2012) 244–252.
[9] S. Mandal, N. Mallick, Microalga Scenedesmus obliquus as a potential source for biodiesel production, Appl. Microbiol. Biotechnol. 84 (2009) 281–291.
[10] L. De Jaeger, R.E.M. Verbeek, R.B. Draaisma, D.E. Martens, J. Springer, G. Eggink, et al., Superior triacylglycerol (TAG) accumulation in starchless mutants of Scenedesmus obliquus: (I) mutant generation and characterization, Biotechnol. Biofuels 7 (2014) 69, https://doi.org/10.1186/1754-6834-7-69.
[11] G. Breuer, L. de Jaeger, V.G.P.G. Artus, D.E. Martens, J. Springer, R.B. Draaisma, et al., Superior triacylglycerol (TAG) accumulation in starchless mutants of Scenedesmus obliquus: (II) evaluation of TAG yield and productivity in controlled photobioreactors, Biotechnol. Biofuels 7 (2014) 1–11, https://doi.org/10.1186/1754-6834-7-70.
[12] B.M. Carreres, G.M. León-Saiki, P.J. Schaap, I.M. Remmers, D. van der Veen, V.A.P. Martins dos Santos, et al., The diurnal transcriptional landscape of the microalga Tetradesmus obliquus, Algal Res. 40 (2019) 101477, , https://doi.org/10.1016/J.ALGAL.2019.101477.
[13] G.M. León-Saiki, T.C. Martí, D. van der Veen, R.H. Wijffels, D.E. Martens, The impact of day length on cell division and efficiency of light use in a starchless mutant of Tetradesmus obliquus, Algal Res. 31 (2018) 387–394.
[14] K.J.M. Mulders, P.P. Lamers, R.H. Wijffels, D.E. Martens, Dynamics of biomass composition and growth during recovery of nitrogen-starved Chromochloris zofingiensis, Appl. Microbiol. Biotechnol. 99 (2014) 1873–1884.
[15] I.M. Remmers, A. Hidalgo-Ulloa, B.P. Brandt, W.A.C. Evers, R.H. Wijffels, P.P. Lamers, Continuous versus batch production of lipids in the microalgae Acutodesmus obliquus, Bioresour. Technol. 244 (2017) 1384–1392.
[16] A.J. Klok, J.A. Verbaanderd, P.P. Lamers, D.E. Martens, A. Rinzema, R.H. Wijffels, A model for customising biomass composition in continuous microalgae production, Bioresour. Technol. 146 (2013) 89–100.
[17] A.M.J. Kliphuis, A.J. Klok, D.E. Martens, P.P. Lamers, M. Janssen, R.H. Wijffels, Metabolic modeling of Chlamydomonas reinhardtii: energy requirements for photoautotrophic growth and maintenance, J. Appl. Phycol. 24 (2012) 253–266, https://doi.org/10.1007/s10811-011-9674-3.
[18] M. DuBois, K.A. Gilles, J.K. Hamilton, P.A. Rebers, F. Smith, Colorimetric method for determination of sugars and related substances, Anal. Chem. 28 (1956) 350–356, https://doi.org/10.1021/ac60111a017.
[19] D. Herbert, P.J. Phipps, R.E. Strange, Chemical analysis of microbial cells, in: J.R. Norris, D.W. Ribbons (Eds.), Methods in Microbiology, vol. 5B, 1971.
[20] P. Postma, T. Miron, G. Olivieri, M.J. Barbosa, R.H. Wijffels, M.H.M. Eppink, Mild disintegration of the green microalgae Chlorella vulgaris using bead milling, Bioresour. Technol. 184 (2015) 297–304.
[21] G. Breuer, P.P. Lamers, M. Janssen, R.H. Wijffels, D.E. Martens, Opportunities to improve the areal oil productivity of microalgae, Bioresour. Technol. 186 (2015) 294–302 (Elsevier).
[22] B.M. Carreres, L. de Jaeger, J. Springer, M.J. Barbosa, G. Breuer, E.J. van den End, et al., Draft genome sequence of the oleaginous green alga *Tetradesmus obliquus* UTEX 393, Genome Announc. 5 (2017) e01449-16, https://doi.org/10.1128/genomeA.01449-16.
[23] M.J. Nueda, S. Tarazona, A. Conesa, Next maSigPro: updating maSigPro bioconductor package for RNA-seq time series, Bioinformatics 30 (2014) 2598–2602.
[24] C. Hennig, fpc: flexible procedures for clustering, https://cran.r-project.org/package=fpc, (2018).
[25] G. Breuer, P.P. Lamers, D.E. Martens, R.B. Draaisma, R.H. Wijffels, The impact of nitrogen starvation on the dynamics of triacylglycerol accumulation in nine microalgae strains, Bioresour. Technol. 124 (2012) 217–226.
[26] Q. Hu, M. Sommerfeld, E. Jarvis, M. Ghirardi, M. Posewitz, M. Seibert, et al., Microalgal triacylglycerols as feedstocks for biofuel production: perspectives and advances, Plant J. 54 (2008) 621–639, https://doi.org/10.1111/j.1365-313X.2008.03492.x.
[27] J. Fan, C. Yan, C. Andre, J. Shanklin, J. Schwender, C. Xu, Oil accumulation is controlled by carbon precursor supply for fatty acid synthesis in *Chlamydomonas reinhardtii*, Plant Cell Phisiol. 53 (2012) 1380–1390.
[28] J.M. Berg, J.L.S.L. Tymoczko, Triacylglycerols are highly concentrated energy stores, Biochemistry, 2002.
[29] C. Lancelot, S. Mathot, Biochemical fractionation of primary production by phytoplankton in Belgian coastal waters during short- and long-term incubations with14C-bicarbonate - I. Mixed diatom population, Mar. Biol. 86 (1985) 219–226.
[30] X. Johnson, J. Alric, Central carbon metabolism and electron transport in Chlamydomonas reinhardtii, metabolic constraints for carbon partitioning between oil and starch, Eukaryot. Cell 12 (6) (2013) 776–793.
[31] Y. Li, D. Han, G. Hu, M. Sommerfeld, Q. Hu, Inhibition of starch synthesis results in overproduction of lipids in Chlamydomonas reinhardtii, Biotechnol. Bioeng. 107 (2010) 258–268, https://doi.org/10.1002/bit.22807.
[32] L. de Jaeger, Strain Improvement of Oleaginous Microalgae, Wageningen University, 2015.
[33] K.E. Baker, R. Parker, Nonsense-mediated mRNA decay: terminating erroneous gene expression, Curr. Opin. Cell Biol. 16 (2004) 293–299, https://doi.org/10.1016/J.CEB.2004.03.003.
[34] L.E. Maquat, Nonsense-mediated mRNA decay: splicing, translation and mRNP dynamics, Nat. Rev. Mol. Cell Biol. 5 (2004) 89–99, https://doi.org/10.1038/nrm1310.
[35] C. Bagnato, M.B. Prados, G.R. Franchini, N. Scaglia, S.E. Miranda, M.V. Beligni, Analysis of triglyceride synthesis unveils a green algal soluble diacylglycerol acyltransferase and provides clues to potential enzymatic components of the chloroplast pathway, BMC Genomics 18 (2017) 1–23.
[36] K. Yoon, D. Han, Y. Li, M. Sommerfeld, Q. Hu, Phospholipid:diacylglycerol acyltransferase is a multifunctional enzyme involved in membrane lipid turnover and degradation while synthesizing triacylglycerol in the unicellular green microalga Chlamydomonas reinhardtii, Plant Cell 24 (2012) 3708–3724, https://doi.org/10.1105/tpc.112.100701.
[37] F. Kong, I.T. Romero, J. Warakanont, Y. Li-Beisson, Lipid catabolism in microalgae, New Phytol. 218 (2018) 1340–1348, https://doi.org/10.1111/nph.15047.
[38] E.L. Rylott, M.A. Hooks, I.A. Graham, Co-ordinate regulation of genes involved in storage lipid mobilization in Arabidopsis thaliana, Biochem. Soc. Trans. 29 (Pt 2) (2001) 283–287.
[39] C.D. Richter, J.W.A. Allen, C.W. Higham, A. Koppenhofer, R.S. Zajicek, N.J. Watmough, et al., Cytochrome cd1, reductive activation and kinetic analysis of a multifunctional respiratory enzyme, J. Biol. Chem. 277 (2002) 3093–3100, https://doi.org/10.1074/jbc.M108944200.
[40] J.A. Hellebust, I. Ahmad, Regulation of nitrogen assimilation in green microalgae, Biol. Oceanogr. 6 (1989) 241–255.
[41] R.J. Cooke, Protein degradation in plants, Sci. Prog. 67 (1981) 461–480, https://doi.org/10.2307/43420541 (1933-).
[42] R.J. Geider, B.A. Osborne, Respiration and microalgal growth: a review of the quantitative relationship between dark respiration and growth, New Phytol. 112 (1989) 327–341.
[43] R.D.E. Visser, C.J.T. Spitters, T.J. Bouma, Energy cost of protein turnover: theoretical calculation and experimental estimation from regression of respiration on protein concentration of full-grown leaves, in: H. Lambers, L.H.W. van der Plas (Eds.), Molecular, Biochemical and Physiological Aspects of Plant Respiration, SPB Academic Publishing bv, The Hague, The Netherlands, 1992, pp. 493–508 ©.
[44] F.W.T. Penning De Vries, The cost of maintenance processes in plant cells, Ann. Bot. 39 (1975) 77–92.